Optical properties of PbTe and PbSe

Chinedu E. Ekuma,[1] David J. Singh,[2] J. Moreno,[1] and M. Jarrell[1]
[1]*Department of Physics and Astronomy, Louisiana State University, Baton Rouge, Louisiana 70803, USA*
[2]*Materials Science and Technology Division, Oak Ridge National Laboratory, Oak Ridge, Tennessee 37831-6056, USA*
(Received 13 November 2011; published 13 February 2012)

We report optical properties of PbTe and PbSe as obtained from first-principles calculations with the Tran-Blaha modified Becke-Johnson potential. The results are discussed in relation to existing experimental data, particularly in relation to the temperature dependence of the band gap.

DOI: 10.1103/PhysRevB.85.085205 PACS number(s): 78.20.Ci, 78.66.Jg, 71.20.−b

I. INTRODUCTION

The narrow-gap IV-VI semiconductors PbX (X = Se, Te) and their alloys have been studied extensively over the past decades,[1–4] motivated in part by interest in PbTe as a thermoelectric material.[5–7] Besides thermoelectrics, lead chalcogenides have been studies for infrared diodes,[8] spintronics,[9] optoelectronics,[10] ferroelectricity,[11] and infrared quantum dot lasers based on PbSe/PbEuTe.[12] Understanding the electronic structure is important for all of these properties and applications. This is particularly important for the thermoelectric properties where electrical transport properties (thermopower and conductivity) that depend on doping and temperature must be optimized.

The basic features of the band structures are known both from experiment (see below, and also, e.g., Refs. 13 and 14) and first-principles calculations.[15–23] Aspects that are clear are: (i) there is a direct band gap at the L point of the Brillouin zone; (ii) both the valence and conduction bands are highly nonparabolic and deviate very substantially from both parabolic band models and Kane models at energies of relevance for their thermoelectric properties; and (iii) there is a secondary feature in the valence band also at energies relevant to thermoelectric properties.

Thermoelectric performance, measured by the figure of merit $ZT = \sigma S^2 T/\kappa$ (σ is electrical conductivity, S is the Seebeck coefficient, and κ is thermal conductivity) is generally a strong function of doping and temperature T. Therefore, obtaining high ZT requires optimization of the doping level. Traditionally, this optimization has been guided by transport models that depend on knowledge of the band structure. In this regard, models for transport in the Pb chalocogenides have been developed and used for many years. These models, which have been capable of describing transport and other data, incorporate various scattering mechanisms and temperature-dependent band structures.[13,14] The conventional model of the valence bands is a two-band model, with a light band maximum at the L point and a heavy band, with strong and different T dependencies for these two bands. This is based on transport and other data, particularly optical measurements indicating a strong, unusual T dependence of the band gap.[24–26]

However, even though these materials, especially PbTe, have been studied for more than 50 years, there have been recent surprises. These include the discovery that even though PbSe was long thought to be much inferior to PbTe, in fact with appropriate doping it can be an excellent thermoelectric material, comparable in performance to PbTe,[27] and that appropriately doped PbTe can be much better than had been previously thought with a ZT well in excess of 1.5.[28] While these results can be rationalized within the conventional two-band models with choices of parameters, specifically relating to the relative positions of the two bands,[27] they were not anticipated by these models and in fact it had been concluded that the high performance found in Tl-doped PbTe was due to special physics associated with Tl (i.e., a resonant level).[29] On the other hand, these results were at least qualitatively anticipated by transport calculations using first-principles band structures,[20,21] and no resonance was found in high-resolution angle-resolved photoemission spectroscopy (ARPES) experiments on Tl-doped PbTe, which instead showed conventional doping behavior.[30]

The underlying first-principles band structure has some commonalities with these models, but is different in essential aspects. The purpose of this paper is to present optical properties of PbTe and PbSe as obtained from the modern band structure as calculated with the recently developed potential functional of Tran and Blaha.[31] This functional (denoted TB-mBJ here)[32] yields band gaps in good accord with experiment,[31,33–35] in contrast to standard density functionals. Therefore the TB-mBJ potential functional enables direct, quantitative comparisons of band structures and optical properties with experiment, without any adjustments, such as scaling the magnitude of the absorption or applying scissors operators to fix the gap. We extensively discuss the results in relation to experimental data. We hope that they will motivate future experimental investigations of the band structure of PbSe and PbTe, particularly using optical measurements and photoemission.

II. APPROACH

Aside from the use of the TB-mBJ potential, the other details of our calculations are standard. We used the general potential linearized augmented planewave (LAPW) method,[36] as implemented in the WIEN2k code.[37] We used well-converged basis sets with dense Brillouin zone samplings, which are needed for the optical properties. For this purpose we used a uniform $48 \times 48 \times 48$ grid. The LAPW sphere radii were 2.75 bohr for both atoms in PbSe and 2.9 bohr for PbTe. We used the experimental rock-salt crystal structure with lattice parameters of 6.464 Å[38] and 6.124 Å[39] for PbTe and PbSe, respectively. All calculations were performed relativistically including spin-orbit coupling (SOC), which is important for

 ©2012 American Physical Society

the band structures of these materials.[16] As mentioned, we apply no scissors operators or other adjustments.

III. BAND STRUCTURE

We begin with the calculated band structures in relation to experimental data. Our calculated band structures for PbSe and PbTe are given in Figs. 1 and 2, respectively. The band structures are qualitatively similar to those reported previously, but there are quantitative differences resulting from the use of the TB-mBJ functional, and these are important.

First of all, we note the values of the band gap. We find band gaps $E_g = 0.36$ eV for PbTe and $E_g = 0.28$ eV for PbSe. The value for PbSe is in good agreement with reported ambient temperature experimental values of 0.27–0.31 eV.[40–43] The calculated gap for PbTe is also in accord with the experimentally reported ambient temperature gap of 0.28–0.36 eV,[44,45] but not the reported low-temperature gap of 0.19 eV. Prior density functional calculations for PbTe, using standard energy functionals, yielded smaller gap values from–0.01–0.25 eV.[18,46–50] The reported density functional band gaps for PbSe range from–0.07–0.18 eV.[18,46–50]

We did calculations as a function of lattice parameters. According to these the 0.24% increase in lattice parameter[51] for PbTe between 120 K and 298 K would yield a band gap change of ∼0.02 eV with the TB-mBJ potential (the band gap increases with increasing lattice parameter). This is too little to explain the difference between our result and the reported low-temperature gap of PbTe even if the lattice expansion is increased by a factor of ∼2 as in some reports.[2] We also carefully checked the dependence of the gap on various computational parameters, such as energy cutoffs, energy window size for the SOC calculation, LAPW sphere radii, and Brillouin zone sampling. We find that at worst the errors related to these are less than 0.03 eV in the gap.

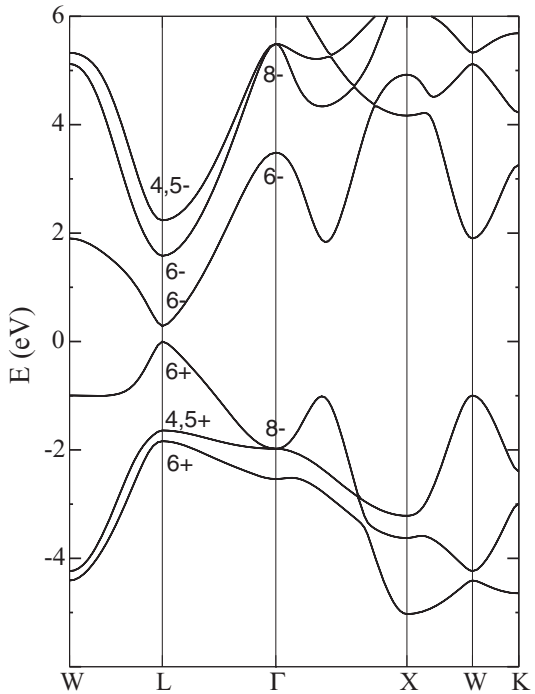

FIG. 1. Calculated band structure of PbSe using the TB-mBJ potential.

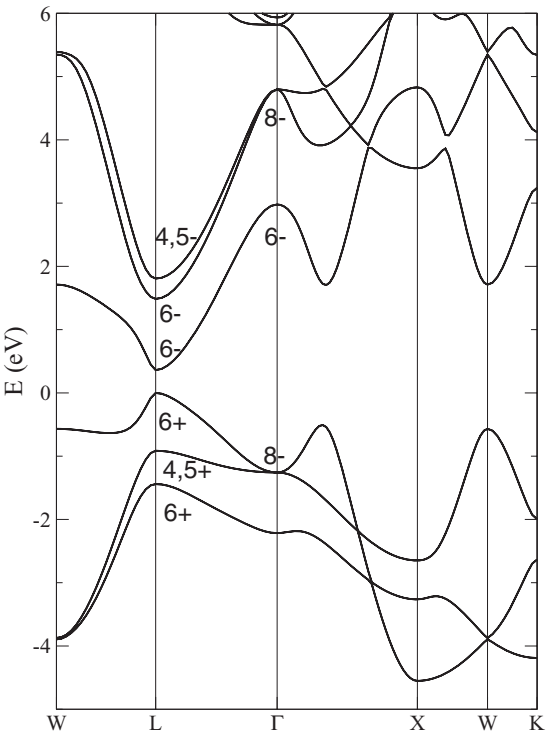

FIG. 2. Calculated band structure of PbTe using the TB-mBJ potential.

The dependence of the gaps on pressure is anomalous in both PbTe and PbSe. The band gap decreases under pressure, while in normal semiconductors it increases. As was discussed by Wei and Zunger,[16] and by Svane and coworkers,[23] this is a consequence of the band ordering at the L point, which depends on spin orbit. This is reproduced in our calculations with the TB-mBJ potential. We find that a 1% compression of the lattice parameter leads to a 0.08 eV decrease in the band gap for PbTe and a 0.11 eV decrease for PbSe, showing the correct band ordering.

The gaps are direct and at the L point in both materials. The bands making up band edges at L are highly nonparabolic and symmetric between electrons and holes, as expected for a Kane band system. This means that, at least close to the band edge, the effective band mass for transport or optics will decrease with increasing energy away from the band edge. However, as energy is increased the bands curve outwards, starting at ∼0.1 eV from the valence band edge, which is reflected in an increase in the density of states (DOS) (Figs. 3 and 4) with increasing binding energy, particularly for the valence bands, where this outward curvature is strongest (note the L-W line, where there is an anticrossing and a rather flat upward dispersion of the highest occupied band approaching W). This feature and its energy position are in close accord with angle-integrated photoemission experiments for PbTe.[30] We note that these measurements were at low temperature, $T = 20$ K. According to their angle-resolved measurements the valence band maximum, again at 20 K, is at a point in the two-dimensional (2D) surface Brillouin zone that corresponds to the L point.

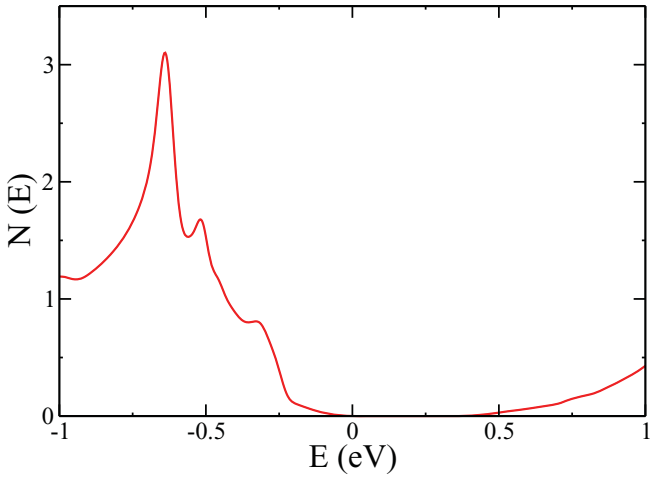

FIG. 3. (Color online) Calculated density of states of PbTe with the TB-mBJ potential.

This outward curvature would be expected to enhance the optical absorption as energy is increased. There is a strong increase in density of states, which has implications for the thermoelectric properties,[20,21] starting at ∼0.2 eV from the valence band edge. This is associated with the connection of the L-point pockets along the lines joining them in the band structure, as discussed previously.[20] Strictly speaking, this reconnection is a topological change in the iso-energy surfaces with binding energy, and not a second band. We note that this is qualitatively the same as the valence band structure of the related compound SnTe, which is seen both from first-principles calculations and detailed ARPES studies,[52,53] and that our band structures are qualitatively similar to those obtained previously,[16,21,46,49,54] although the gap and band energies differ reflecting our use of the TB-mBJ potential.

IV. COMPARISON WITH ANGLE-RESOLVED PHOTOEMISSION SPECTROSCOPY

ARPES experiments provide a direct measure of the electronic structure of the occupied states and, as mentioned, have been recently applied to establish an electronic structure for SnTe in accord with band structure predictions.[52] There have also been ARPES experiments for PbSe and PbTe, with which we can compare.[30,55–57]

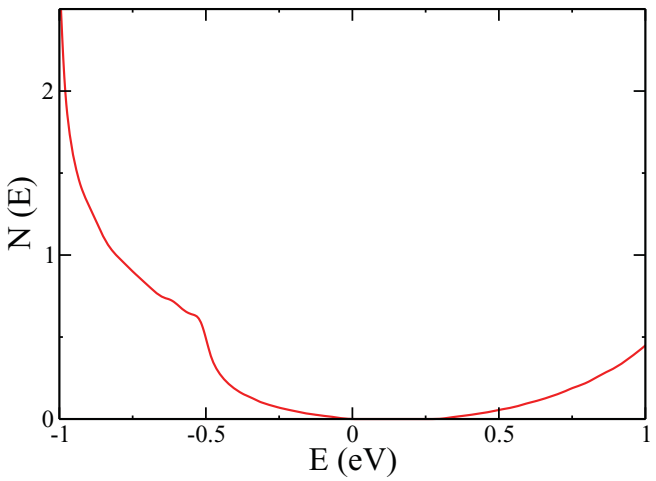

FIG. 4. (Color online) Calculated density of states of PbSe with the TB-mBJ potential.

While the bands are actually derived from hybridized Pb $6p$ and Te $5p$ states, the conduction bands are formed mainly by the Pb $6p$ states. Due to SOC, one conduction band is lowered in energy at the Γ point. According to our calculations, the spin-orbit splitting (SOS) of Pb $6p$ states (i.e., $\Gamma_6^- - \Gamma_8^-$ splitting, with the notation of Herman[58]) is calculated to be 1.8 eV in PbTe and 2.0 eV in PbSe. The conduction band SOS defined by the splitting of the second and third conduction bands, which comes from the second conduction band at Γ (Γ_8^-) are 0.31 and 0.05 eV for PbTe at W and L points, respectively, while the SOS for PbSe are 0.21 and 0.66 eV at W and L points, respectively.

The hybridization between Pb $6p$ and anion p states contributed significantly to the SOS of the valence bands. For PbTe, the SOS is 0.52 eV at the L point (i.e., $L_6^+ - L_{45}^+$ splitting), 1.05 eV at the Γ point (i.e., $\Gamma_6^- - \Gamma_8^-$), and 1.10 eV at X (i.e., $X_6^- - X_6^-$). The Δ_6(max) is calculated to be 0.54 eV. These values are in excellent agreement with experiment. Angle-resolved photoemission experiments[55,56] found values of 1.10–1.15 eV, 0.90–1.10 eV, and 0.3–0.7 eV at the Γ, X points, and the Δ_6(max) value, respectively.

The SOS of PbSe is somewhat different from that of PbTe. The calculated SOS is 0.20 eV at the W point, 0.21 eV at L, 0.55 eV at the Γ point, 1.32 eV at the X point, and Δ_6(max) value of 0.99 eV. We note that the SOS values are in very good agreement with angle-resolved photoemission experiments[55,56] except for the SOS at the X point. These authors found values of 0.60–0.75 eV at the Γ, 0.5–0.55 eV at the X point, and Δ_6(max) value of 0.6–1.1 eV. It is not clear what the reason for the discrepancy at X is. We note that since the SOS of both PbTe and PbSe share relatively the same features, they are not expected to be too different from each other as seen both in the calculated and experimental values of the SOS. It may be noted that the bands close to Δ before X on the high-symmetry points (see Figs. 2 and 1) anticross with the upper L_6^+ band, which could make distinguishing between the different bands difficult. In both systems, the L_6^+ band at the high-symmetry points of the Brillouin zone (BZ) is nondegenerate.

V. OPTICAL PROPERTIES AND COMPARISON WITH EXPERIMENT

Optical spectroscopy, while less direct than ARPES, provides detailed information about the electronic structure and has the advantage of being a true bulk probe. There have been a number of optical studies of PbSe and PbTe, both on bulk crystals and on thin films.[1–4,25,45,59–64]

As mentioned, we calculated optical properties based on our TB-mBJ electronic structure with no adjustment. This was done using the optical properties package of the WIEN2k code. While it is conventional to plot calculated optical data with a broadening added to mimic experimental data, we instead show results with no added broadening in order to show more clearly the features in the calculated spectra. The calculated absorption spectra are shown in Fig. 5. Our absorptive parts

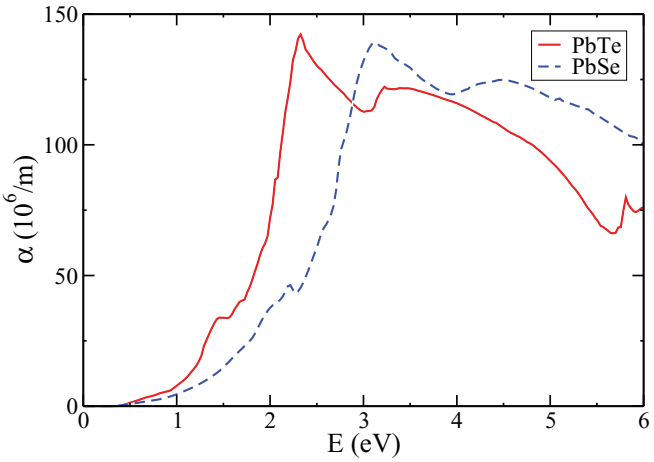

FIG. 5. (Color online) Calculated optical absorption $\alpha(\omega)$ without broadening.

of the dielectric constant of PbTe and PbSe are shown in Fig. 6.

In discussing these it is helpful to divide the energy range into a high-energy region above 1 eV and the region below 1 eV, which is the near-band-edge region. Both regions have been studied though generally not in the same experiment. Experiments in the high-energy region both with thermoreflectance and critical point analysis have been done. Optical spectra obtained from standard density functional calculations show good accord with these as regards the overall shape of the spectra to the relative positions of critical points.[49,50,65] The situation for the energy range below 1 eV (i.e., the range relevant to transport) is more complex. The general understanding in the literature is that there are two valence bands in proximity to the Fermi energy, and that, as mentioned, at least one of them shows a strong complex temperature dependence in PbTe.[25,26] In particular, the band gap for PbTe is quoted as ∼0.19 eV at 0 K, increasing linearly with T to ∼0.36 eV at ∼400 K and then becoming constant at higher T above ∼450 K.

This picture is supported by almost all optical experiments reported to date, although the actual data reported in different

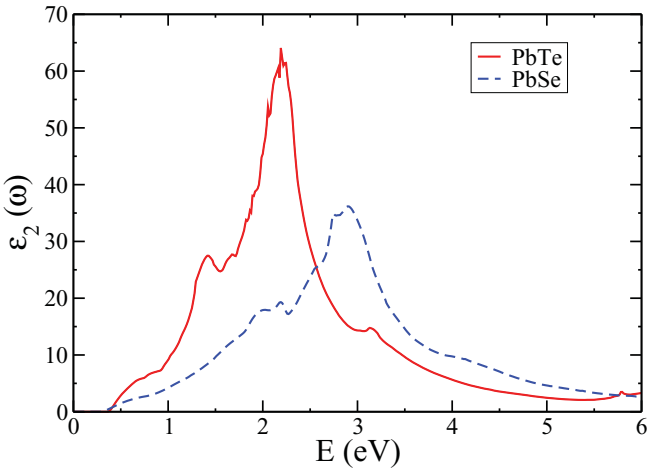

FIG. 6. (Color online) Calculated imaginary part $\varepsilon_2(\omega)$ of the dielectric function without broadening.

papers varies (see, e.g., the data of Refs. 25, 45 and 63, in relation to each other), which could suggest an extrinsic origin for the low T absorption at energies below the high-temperature band edge (∼0.36 eV).

On the other hand, it is known that PbTe is in proximity to a ferroelectric instability. As such, unusual phonon behavior as a function of T and pressure occurs,[66–68] which perhaps could lead to unusual T dependence and pressure dependence of the band gap through the electron-phonon coupling. In fact Tsang and Cohen[26] presented a model for the T dependence based on electron-phonon coupling and an empirically parametrized pseudopotential.[26] This model cannot explain the change in behavior at ∼450 K. The situation is complicated by the fact that in pure PbTe, free carriers are introduced into the valence band by the formation of Pb vacancies,[69,70] and in general it is difficult to obtain pure intrinsic PbSe and PbTe (note that high resistivity does not imply defect-free material, as high resistivity can be obtained by carrier compensation and Fermi level pinning due to defects).[47,48]

The optical properties of PbTe and PbSe have been studied using several experimental methods.[1–4,59–62,64] Most of the studies in the visible and ultraviolet have been near-normal incidence reflectivity measurements.[60] These methods have certain potential sources of errors. In general, they involve multiple measurements to obtain the dielectric constants and/or Kramers-Kronig (KK) analysis, which can suffer from uncertainty in the absolute amplitude. This is associated with extrapolations necessary for the KK transformation of experimental reflectivity spectra.

Spectroscopic ellipsometry (SE) is one of the parallel measurement techniques that avoids these problems in measuring the optical constants of solids.[71] The big advantage of the SE technique, and other parallel measurement techniques, is that both the real and imaginary part of the complex dielectric function of a material may be obtained directly as a function of wavelength without requiring multiple measurements or KK analysis. Some of the earliest SE measurements for PbTe and PbSe were those of Suzuki and coworkers.[40,59] Globus and coworkers,[72] using the parallel measurement of the optical transmission studied the dielectric function of PbSe in a more narrow range. We reiterate that none of our spectra were shifted to coincide with experiment contrary to what is often done in such comparisons with experiments (e.g., Ref. 50 where $\varepsilon_2(\omega)$ was shifted by 0.3 eV for PbSe and 0.15 eV for PbTe).

The $\varepsilon_2(\omega)$ spectra for both materials share the same characteristic features. In PbTe, we found a shoulder around 1.40 eV, followed by another set of close shoulders around 2.0 eV. A broad shoulder is found near 3.15 eV. The maximum for $\varepsilon_2(\omega)$ is ∼63.0 at energy of 2.20 eV. Our $\varepsilon_2(\omega)$ spectra are in excellent agreement with the SE data of Suzuki and coworkers.[59] Their SE measurements show a shoulder around 1.5 eV and maximum amplitude for $\varepsilon_2(\omega)$ of ∼54. For PbSe, we obtain a shoulder at 1.95 eV and a maximum amplitude of $\varepsilon_2(\omega)$ of 36.1 at 2.89 eV. We also find a shoulder at 4.04 eV. Our computed values are also in excellent accord with experiment. The data of Ref. 40 show a shoulder around 1.60 eV, maximum amplitude of $\varepsilon_2(\omega)$ around 36.0 at energy of 2.73 eV, and a relatively broader shoulder just as in our case at ∼4.10 eV. We emphasize that we have not employed any shift or scissors

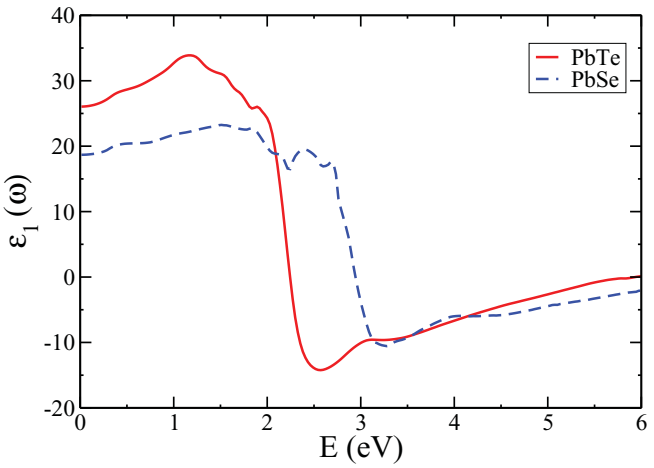

FIG. 7. (Color online) Calculated real part of the dielectric function without broadening.

operator but have directly calculated the optical spectra from the TB-mBJ band structure.

Our calculated dispersive parts of the dielectric function, $\varepsilon_1(\omega)$, for PbTe and PbSe are shown in Fig. 7. The main experimental features in PbSe and PbTe[40,59] are reproduced in our results. The main features in both PbTe and PbSe are shoulders at 1.85–2.6 eV, followed by a steep decrease at ∼2.02 eV for PbTe and ∼2.70 eV for PbSe. Then, $\varepsilon_1(\omega)$ becomes negative, with a minimum at ∼2.56 eV for PbTe and ∼3.24 eV for PbSe, before slowly increasing toward zero at higher energies. The maximum amplitude of $\varepsilon_1(\omega)$ in PbTe is 34.1 at 1.15 eV, while in PbSe it is 23.3 at 1.50 eV. Our computed maximum amplitude is in good accord with the experimental values of ∼36 for PbTe[59] and ∼24 for PbSe.[40]

The maximum amplitudes of the absorption spectra are 137×10^6 m^{-1} and 133×10^6 m^{-1} for PbTe and PbSe, respectively. This is in good accord with reported SE data for PbTe[59,64] and PbSe.[40]

Thus in the high-energy (1 eV and up) region there is a very close correspondence between our first-principles results, which represent standard band structure descriptions, and both optical data from SE and ARPES measurements and this is equally the case for both PbTe and PbSe. We now turn to the low-energy region focusing on PbTe.

VI. DISCUSSION

As mentioned, it is generally held that the band gap of PbTe is strongly T dependent up to ∼400 K becoming constant for T above ∼450 K. This picture is based on optical data, which we now briefly review. Gibson reported absorption and photoconductivity measurements for doped PbS, PbSe, and PbTe samples, finding a strongly T-dependent absorption edge in all three materials, with an onset of photoconductivity at this edge.[73] He associated this edge with the band gap, finding a linear dependence of the gap from 20 K, which was the lowest temperature measured, up to ∼450 K for PbTe, with very similar behavior in PbS and PbSe. His direct absorption measurements extended up to maximum absorption values of $\alpha \sim 100$ cm^{-1} in PbS, $\alpha \sim 170$ cm^{-1} in PbSe, and $\alpha \sim 280$ cm^{-1} in PbTe. All his data have an upward curvature as wavelength is decreased (energy increased).

Miller, Komarek, and Cadoff (MKC) measured transport data and optical absorption data at 300 K for PbTe.[24] Their measurements included Hall, Seebeck, and resistivity. They show very clean transport data and note that the gap value extracted from this cannot be reconciled with the absorption data. They showed absorption data at room temperature, showing a very good fit to the expected $\alpha \propto (E - E_g)^2$, which is the form appropriate to an indirect band gap. This shape is qualitatively similar to that reported by Gibson, who, as mentioned, found an upward curvature. We note that the band gap of PbTe is now known to be direct, for which the shape, at least at low energy, of $\alpha \propto (E - E_g)^{1/2}$ is expected. Also, we note that MKC state that they used a spectrometer slit width of 0.007 eV (7 meV) and show data over an energy range of only 0.02 eV from the absorption onset (i.e., less than three times the slit width). The maximum value of the absorption they report is $\alpha \sim 225$ cm^{-1}. They reconcile their transport and optical data in favor of the optical data, concluding very similarly to Gibson that the gap is small compared to the high-T value and that the transport data is affected by the formation of defects.

A subsequent study by Tauber, Machonis, and Cadoff (TMC) shows very similar data at various T from 93–515 K, with a similar conclusion. They only show data up to $\alpha \sim 300$ cm^{-1} and with the exception of the high-temperature data, only over the same very small energy ranges. At high T above 450 K, their absorption spectra show a higher onset that is weakly T dependent, but the curves have a weaker energy dependence. By 515 K, they find a downward curvature of $\alpha(E)$, which is the expected behavior of a direct gap. In any case, TMC conclude that PbTe has a strongly T-dependent indirect band gap. As the previous study of Gibson,[73] they find this absorption edge above a relatively flat and low background absorption, of less than 50 cm^{-1}, in contrast to the Urbach tail that is expected even in very high-quality semiconductor samples below the strong absorption edge associated with a band gap.

More recently, Wang and coworkers[64] carried out an extensive infrared SE study of PbTe thick films in the wavelength range of 2–8 μm. They found a band gap of 0.386 eV, with a normal Urbach tail and the proper $(E - E_g)^{1/2}$ energy dependence for a direct gap. They ascribed the fact that their value of the band gap is higher than that reported for $T = 300$ K by MKC and TMC to quantum confinement associated with the nanocrystalline nature of their films, which according to scanning probe measurements have a distribution of grain sizes in the range 50–100 nm. We note that their gap value is consistent with both our TB-mBJ value and the high-temperature value from older literature as discussed above and, as mentioned, in contrast to the conclusion of MKC and TMC the gap is direct. It should also be pointed out that PbTe tends to form with substantial defect concentrations and it is very difficult to obtain undoped, intrinsic PbTe.[14,69,70] Therefore, one could reconcile the various data by assuming not that the band gap is T dependent, but that there are defect states that occur near midgap at low T in PbTe. Such deep trap states would tend to pin the Fermi level in otherwise near stoichiometric material and would have the effect of strongly increasing resistivity. Such midgap traps are now understood to

be one of the few ways to obtain high resistivity in compound semiconductors that have low defect formation energies, such as PbTe, while in the earlier work of Cadoff and collaborators, high resistivity was emphasized as an indicator of high sample quality in analogy with elemental semiconductors, such as Ge.

Therefore, we propose that the experimental data, which has been interpreted in terms of an anomalous temperature dependence of the band gap in the Pb chalcogenides could alternatively be interpreted as a defect level near midgap in PbTe, that shifts closer to one of the band edges with temperature. This would be consistent with the nondirect energy dependence of the absorption spectra reported by Cadoff and coworkers, the more recent SE measurements of Wang and coworkers,[64] and the return to weakly T-dependent behavior at temperatures above 450 K, where even if it did not enter the band edge, such a trap state would be thermally depopulated. It is also consistent with the association of absorption and photoconductivity, since optical excitation of a carrier trap state normally leads to increased conductivity. Furthermore, we point out that the low-energy shape of our calculated DOS, which has the band maximum at L and the higher-energy binding energy feature due to connection of the L-point pockets agrees with the structure of low temperature photoemission experiments.[30]

While we emphasize that none of the above discussion proves that an alternative picture in terms of midgap defect states is correct, we hope that it motivates experimental work using modern spectroscopy to test the existing model of strongly temperature-dependent band structures in PbTe and PbSe. This could be done by modern SE measurements over a wider energy range, temperature-dependent ARPES, and perhaps other methods.

ACKNOWLEDGMENTS

We are grateful for helpful discussions with John Cerne. Work at Oak Ridge National Laboratory (ORNL) was supported by the Department of Energy, Basic Energy Sciences through the S3TEC Energy Frontier Research Center. Work at Louisiana State University (LSU) was funded in part by the National Science Foundation, Award No. EPS 1003897. High-performance computational resources were provided by the Louisiana Optical Network Initiative (LONI). C.E.E. thanks Ebonyi State, Federal Republic of Nigeria.

[1] W. D. Lawson, J. Appl. Phys. **22**, 1444 (1951).
[2] Y. W. Tung and M. L. Cohen, Phys. Rev. B **180**, 823 (1969).
[3] S. E. Kohn, P. Y. Yu, Y. Petroff, Y. R. Shen, Y. Tsang, and M. L. Cohen, Phys. Rev. B **8**, 1477 (1973).
[4] R. Dalven, in *Solid State Physics*, edited by H. Ehrenreich, F. Seitz and D. Turnbull (Academic, New York, 1973), Vol. 28.
[5] A. F. Ioffe, *Semiconductor Thermoelements and Thermoelectric Cooling* (Inforsearch, London, 1957).
[6] C. Wood, Rep. Prog. Phys. **51**, 459 (1988).
[7] D. M. Rowe, *CRC Handbook of Thermoelectrics* (CRC Press, Boca Raton, 1995).
[8] J. John and H. Zogg, J. Appl. Phys. **85**, 3364 (1989).
[9] S. Jin, H. Wu, and T. Xu, J. Appl. Phys. Lett. **95**, 132105 (2009).
[10] B. Akimov, A. Dmitriev, D. Khohlov, and L. Ryabova, Phys. Status Solidi A **137**, 9 (1993).
[11] A. I. Lebedev and I. A. Sluchinskaya, Ferroelectrics **157**, 275 (1994).
[12] G. Springholz, T. Schwarzl, W. Heiss, G. Bauer, H. Aigle, M. Pascher, and I. Vavra, Appl. Phys. Lett. **79**, 1225 (2001).
[13] Y. I. Ravich, B. A. Efimova, and V. I. Tamarchenko, Phys. Status Solidi B **48**, 11 (1971).
[14] Y. I. Ravich, B. A. Efimova, and V. I. Tamarchenko, Phys. Status Solidi B **48**, 453 (1971).
[15] P. J. Lin and L. Kleinman, Phys. Rev. **142**, 478 (1966).
[16] S. H. Wei and A. Zunger, Phys. Rev. B **55**, 13605 (1997).
[17] D. I. Bilc, S. D. Mahanti, and M. G. Kanatzidis, Phys. Rev. B **74**, 125202 (2006).
[18] K. Hummer, A. Gruneis, and G. Kresse, Phys. Rev. B **75**, 195211 (2007).
[19] L. Zhang, A. Grytsiv, P. Rogl, E. Bauer, and M. Zehetbauer, J. Phys. D **42**, 225405 (2009).
[20] D. J. Singh, Phys. Rev. B **81**, 195217 (2010).
[21] D. Parker and D. J. Singh, Phys. Rev. B **82**, 035204 (2010).
[22] L. Q. Xu, Y. P. Zheng, and J. C. Zheng, Phys. Rev. B **82**, 195102 (2010).
[23] A. Svane, N. E. Christensen, M. Cardona, A. N. Chantis, M. van Schilfgaarde, and T. Kotani, Phys. Rev. B **81**, 245120 (2010).
[24] E. Miller, K. Komarek, and I. Cadoff, J. Appl. Phys. **32**, 2457 (1961).
[25] R. N. Tauber, A. A. Machonis, and I. B. Cadoff, J. Appl. Phys. **37**, 4855 (1966).
[26] Y. W. Tsang and M. L. Cohen, Phys. Rev. B **3**, 1254 (1971).
[27] Y. Z. Pei, A. LaLonde, S. Iwanaga, and G. J. Snyder, Energy Environmental Science **4**, 2085 (2011).
[28] H. Wang, Y. Z. Pei, A. D. LaLonde, and G. J. Snyder, Adv. Mater. **23**, 1366 (2011).
[29] J. P. Heremans, V. Joavovic, E. S. Toberer, A. Saramat, K. Kurosaki, A. Charoenphakdee, S. Yamanaka, and G. J. Snyder, Science **321**, 554 (2008).
[30] K. Nakayama, T. Sato, T. Takahashi, and H. Murakami, Phys. Rev. Lett. **100**, 227004 (2008).
[31] F. Tran and P. Blaha, Phys. Rev. Lett. **102**, 226401 (2009).
[32] J. P. Perdew, J. A. Chevary, S. H. Vosko, K. A. Jackson, M. R. Pederson, D. J. Singh, and C. Fiolhais, Phys. Rev. B **46**, 6671 (1992).
[33] D. J. Singh, Phys. Rev. B **82**, 155145 (2010).
[34] D. J. Singh, Phys. Rev. B **82**, 205102 (2010).
[35] D. Koller, F. Tran, and P. Blaha, Phys. Rev. B **83**, 195134 (2011).
[36] D. J. Singh and L. Nordstrom, *Planewaves, Pseudopotentials and the LAPW Method*, 2nd ed. (Springer-Verlag, Berlin, 2006).
[37] P. Blaha, K. Schwarz, G. Madsen, D. Kvasnicka, and J. Luitz, WIEN2k, An Augmented Plane Wave + Local Orbitals Program for Calculating Crystal Properties (K. Schwarz, Technische Universität Wien, Austria, 2001).
[38] P. M. Nikolic, Brit. J. Appl. Phys. **16**, 1075 (1965).
[39] K. Dalven, Infrared Phys. **9**, 141 (1969).

[40]N. Suzuki, K. Sawai, and S. Adachi, J. Appl. Phys. **77**, 1249 (1994).
[41]W. H. Strehlow and E. L. Cook, J. Phys. Chem. Ref. Data **2**, 163 (1973).
[42]O. Madelung, U. Rössler, and M. Schulz, *Semiconductors Non-Tetrahedrally Bonded Elements and Binary Compounds I: Landolt-Bornstein, New Series, Group III*, Vol. 41c (Springer-Verlag, Berlin, 1998).
[43]W. W. Scanlon, in *Solid State Physics*, edited by H. Ehrenreich, F. Seitz and D. Turnbull (Academic, New York, 1959), Vol. 9, p. 83.
[44]U. Schlichting, Ph.D. thesis, Technische Universität Berlin, 1970.
[45]K. V. Narasimham, J. C. Joshi, K. N. Chopra, C. Jagadish, and A. L. Dawar, Infrared Phys. **23**, 349 (1983).
[46]E. A. Albanesi, E. L. Peltzer y Blanca, and A. G. Petukhov, Comput. Mater. Sci. **32**, 85 (2005).
[47]G. Martinez, M. Schluter, and M. L. Cohen, Phys. Rev. B **11**, 660 (1975).
[48]M. Schluter, G. Martinez, and M. L. Cohen, Phys. Rev. B **12**, 650 (1975).
[49]E. A. Albanesi, C. M. I. Okoye, C. O. Rodriguez, E. L. Peltzery Blanca, and A. G. Petukhov, Phys. Rev. B **61**, 16589 (2000).
[50]A. Delin, P. Ravindran, O. Eriksson, and J. M. Wills, Int. J. Quantum Chem. **69**, 349 (1998).
[51]Y. Noda, K. Masumoto, S. Ohba, Y. Saito, K. Toriumi, Y. Iwata, and I. Shibuya, Acta Crystallogr. Sect. C **43**, 1443 (1987).
[52]P. B. Littlewood, B. Mihaila, R. K. Schulze, D. J. Safarik, J. E. Gubernatis, A. Bostwick, E. Rotenberg, C. P. Opeil, T. Durakiewicz, J. L. Smith, and J. C. Lashley, Phys. Rev. Lett. **105**, 086404 (2010).
[53]D. J. Singh, Functional Materials Lett. **3**, 223 (2010).
[54]M. Lach-hab, D. Papaconstantopoulos, and M. J. Mehl, J. Phys. Chem. Solids **63**, 833 (2002).
[55]V. Hinkel, H. Haak, C. Mariani, L. Sorba, K. Horn, and N. E. Christensen, Phys. Rev. B **40**, 5549 (1989).
[56]T. Grandke, L. Ley, and M. Cardona, Phys. Rev. B **18**, 3847 (1978).
[57]T. Grandke, L. Ley, M. Cardona, and H. Preier, Solid State Commun. **24**, 287 (1977).
[58]F. Herman, R. L. Kortum, I. B. Ortenburger, and J. Van Dyke, J. Physique (Suppl.) **29**, 62 (1968).
[59]N. Suzuki, K. Sawai, and S. Adachi, Jpn. J. Appl. Phys. **33**, 193 (1994).
[60]M. Cardona and D. L. Greenaway, Phys. Rev. **133**, A1685 (1964).
[61]T. Moss, *Optical Properties of Semiconductors* (Butterworth, London, 1959).
[62]F. J. Bogacki, A. K. Sood, C. Y. Yang, S. Rabii, and J. E. Fischer, Surf. Sci. **37**, 494 (1973).
[63]N. Piccioli, J. M. Besson, and M. Balkansi, J. Phys. Chem. Solids **35**, 971 (1974).
[64]J. Wang, J. Hu, X. Sun, A. M. Agarwal, L. C. Kimerling, D. R. Lim, and R. A. Synowicki, J. Appl. Phys. **104**, 053707 (2008).
[65]D. Rached, M. Rabah, N. Benkhettou, M. Driz, and B. Soudini, Physica B **337**, 394 (2003).
[66]H. Burkhard, C. Bauer, and A. Lopez-Otero, J. Opt. Soc. Am. **67**, 943 (1997).
[67]J. An, A. Subedi, and D. J. Singh, Solid State Commun. **148**, 417 (2008).
[68]O. Delaire, J. Ma, K. Marty, A. F. May, M. A. McGuire, M. H. Du, D. J. Singh, A. Podlesnyak, G. Ehlers, M. D. Lumsden, and B. C. Sales, Nature Mater. **10**, 614 (2011).
[69]N. J. Parada, Phys. Rev. B **3**, 2042 (1971).
[70]N. J. Parada and G. W. Pratt, Phys. Rev. Lett. **22**, 180 (1969).
[71]D. E. Aspnes, in *Handbook of Optical Constants of Solids*, edited by E. D. Palik (Academic, New York, 1985), p. 89.
[72]T. R. Globus, A. O. Olesk, and S. A. Olesk, Sov. Phys. Semicond. **24**, 22 (1990).
[73]A. F. Gibson, Proc. Phys. Soc. (London) B **65**, 378 (1952).